Int. J. Corros. Scale Inhib., 2015, **4**, no. 1, 57 – 74

Enhanced corrosion inhibition of mild steel in CO_2-saturated solutions containing some novel green surfactants based on cottonseed oil

I. T. Ismayilov,[1,2] Hany M. Abd El-Lateef,[2] V. M. Abbasov,[1] E. N. Efremenko,[3] L. I. Aliyeva[1] and Ch. K. Salmanova[1]

[1]*Mamedaliev Institute of Petrochemical Processes, National Academy of Sciences of Azerbaijan, AZ1025 Baku, Azerbaijan*
[2]*Chemistry Department, Faculty of Science, Sohag University, 82524 Sohag, Egypt*
[3]*Faculty of Chemistry, Lomonosov Moscow State University, 119991, GSP-1, 1-3 Leninskiye Gory, Moscow, Russia*
E-mail: Hany_shubra@yahoo.co.uk

Abstract

Some novel green surfactants based on cottonseed oil were synthesized and tested as inhibitors for the corrosion of mild steel in CO_2-saturated 1% NaCl solution by potentiodynamic polarization and linear polarization resistance corrosion rate measurements at 50°C. Their critical micelle concentrations at equilibrium in water at 25°C were also determined. Inhibition efficiency increased with increase in the concentration of the studied surfactants, reached the maximum (99.34%) at 100 ppm. The Tafel polarization results indicate that the inhibitors act as mixed inhibitors. The adsorption of the inhibitors on the steel surface obeys Langmuir isotherms. The thermodynamic parameters of adsorption revealed a strong interaction between the inhibitors and the corroding mild steel surface.

Keywords: *green surfactants, mild steel, CO_2-saturated solutions, cottonseed oil, inhibition.*

Received: December 22, 2014. doi: 10.17675/2305-6894-2015-4-1-057-074

1. Introduction

The carbon dioxide corrosion of mild steel represents a significant problem for both the oil and gas industries [1−5]**.** Although high cost corrosion resistance alloys were developed to be able to resist the CO_2 corrosion, mild steel is still the most cost effective material used in CO_2 corrosion [4]. The problems of CO_2 corrosion of mild steel were firstly recognized in the 1940's and have been investigated for over 60 years [5]. However, until now the research work in the literature is still confusing and sometime contradictory [5]. Therefore, it is very important to improve the prediction and control of the CO_2 corrosion of mild steel.

The use of inhibitors is one of the most practical methods for protection against corrosion [6–10]. To be effective, an inhibitor must also transfer water from the metal surface, interact with anodic or cathodic reaction sites to retard the oxidation and reduction corrosion reaction, and prevent transportation of water and corrosion-active species on the metal surface. Surfactants, when used as inhibitors, act through a process of surface adsorption. Adsorption of surfactant on solid surfaces can modify the surface charge, and also the hydrophobic and other key properties of the solid surface that influence interfacial processes. In general adsorption is governed by different types of forces, such as covalent bonding, electrostatic attraction, hydrogen bonding, *etc*. [11]. Several studies suggested that most organic surfactant inhibitors are adsorbed on the metal surface by displacing water molecules from the surface and forming a compact barrier film [12]. The ability of a surfactant molecule to adsorb is generally directly related to its ability to aggregate and to form micelles.

In the present work, we describe the synthesis of novel green surfactants inhibitors based on cotton seed oil. Corrosion inhibition of mild steel in CO_2-saturated 1% NaCl solution in the presence of the investigated surfactants has been studied by using the linear polarization resistance corrosion rate and potentiodynamic polarization measurements, and possible adsorption mechanism of the surfactants on metal surface in the corrosive medium is also described.

2. Experimental procedure

2.1. Synthesis of Surfactants

The studied surfactants were synthesized in our laboratory based on cottonseed oil. Cottonseed oil was reacted with monoethanolamine for 15 hours at 150–160°C. These processes produce fatty acid monoethanolamine amide. Based on the last prepared compound sulfating syntheses were performed**.** The product is **s**ulfated fatty acid monoethanolamine amide. Five types from surfactants were synthesized in high purity by the following composition: [R–CH–(OSO_3M)–CONH–CH_2–CH_2–OH] (where M = Na, K, NH_4, –NH–CH_2–CH_2–OH and –N–(CH_2–CH_2–OH)$_2$). List of the synthesized surfactants are shown in Table 1. The chemical structure of the synthesized surfactants was characterized by using FT-IR, Spectrum BX spectrometer using KBr disks.

2.2. Chemical composition of mild steel alloy

Electrodes are made of mild steel grade 080A15 and have an area of 4.55 cm^2. The mechanical properties of the mild steel measured at room temperature were provided by supplier shown as follows: tensile strength equal to 490 MPa and elongation to failure equal to 16%. The Chemical composition of mild steel used in this study was given in Table 2. The data was provided by European Corrosion Supplies Ltd.

2.3. Preparation of solutions

The aggressive solution, 1% NaCl, was prepared by dissolving of analytical grade NaCl in distilled water. The concentration range of the prepared surfactants was from 25 to 100 ppm used for corrosion measurements.

Table 1. List of the synthesized surfactants including code number, name and structure.

Code number of the inhibitor	Name and abbreviation	Structure	Molecular weight (g /mol)
S_I	Sodium salt of sulfated fatty acid monoethanolamine amide (SSFM)	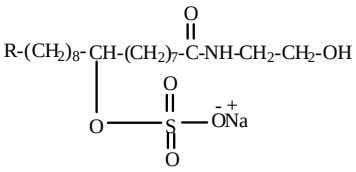	401
S_{II}	Potassium salt of sulfated fatty acid monoethanolamine amide (PSFM)	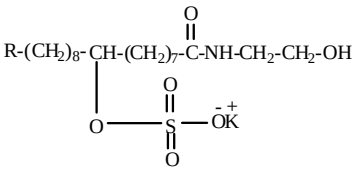	417
S_{III}	Ammonium salt of sulfated fatty acid monoethanolamine amide (ASFM)	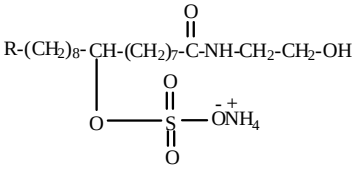	395
S_{IV}	Sulfated fatty acid monoethanolamine amide - monoethanolamine complex (MCFM)	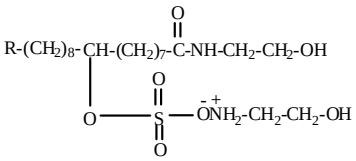	427
S_V	Sulfated fatty acid monoethanolamine amide - diethanolamine Complex (DCFM)	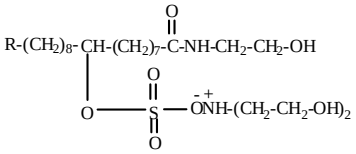	476

Table 2. Chemical composition of mild steel alloy.

Element	Si	Ni	Cr	C	S	P	Mn	Fe
Content, (wt. %)	0.24	0.01	0.10	0.18	0.05	0.05	0.50	Balance

2.4. Corrosion measurements

The measurements were performed on the rotating cylinder electrode. This electrode was used for one time. The reference electrode was Ag/AgCl electrode to which all potentials are referred.

Before beginning the experiment, the prepared 1% sodium chloride solution was stirred by a magnetic stirrer for 60 min in 1000 ml cell. Then this cell was thermostated at a temperature 50°C for 1 hour under a pressure of 0.9 bars. The solution was saturated with carbon dioxide. To remove any surface contamination and air formed oxide, the working electrode was kept at −1500 mV (Ag/AgCl) for 5 min in the tested solution, disconnected shaken free of adsorbed hydrogen bubbles and then cathodic and anodic polarization was recorded. ACM Gill AC instrument connected with a personal computer was used for the measurements.

2.4.1. Potentiodynamic polarization measurements

The extrapolation of cathodic and anodic Tafel lines was carried out in a potential range ±150 mV with respect to corrosion potential (E_{corr}) at scan rate of 1 mV/s.

2.4.2. Linear polarization resistance corrosion rate

LPR corrosion rate bubble-test method involves evaluating the corrosion of a given metal in simulated brine saturated with CO_2 at a temperature equivalent to that in the field. The prepared of 1% NaCl was stirred by a magnetic stirrer for 60 min in 4000 ml. The prepared solution poured into the 4 glass beakers (1000 ml for each one). Then these beakers were placed on a heater at 50°C for 1 hour under a pressure of 0.9 bars of CO_2. The solution was saturated with carbon dioxide. After that, the electrodes were placed in the medium and are connected through a potentiometer ACM GILL AC. The surface of working electrode is cleaned by acetone before using, these electrodes are using for one time. After 1 hour, except for 1 beaker, the remaining 3 is fed with the suitable amount of inhibitor and continued supply of CO_2 under pressure of 0.9 bar until the end of the experiment.

The potential of the working electrode was varied by a CoreRunning programme (Version 5.1.3.) through an ACM instrument Gill AC. The CoreRunning programme converts a corrosion current in mA/cm^2 to a corrosion rate in mm/year. A cylindrical mild steel rod of the composition 080A15 GRADE STEEL was used as a working electrode. Gill AC technology allows measure DC and AC signals using standard Sequencer software. A small sweep from typically –10 mV to +10 mV at 10 mV/min around the rest potential is performed.

2.5. Surface tension measurements

It is of interest to study the micellar properties of solutions of these compounds in order to correlate their surface active properties with critical micelle concentration (CMC). The surface tensions were determined by DuNouy Tensiometer, Kruss Type 8451 and the temperature was maintained precisely at 25°C.

3. Results and Discussions

3.1. Chemical structure of the synthesized surfactants

The structural characteristic of fatty acid monoethanolamine amide before and after sulfating processes was confirmed by FT-IR spectroscopy in the range 4000–500 cm^{-1}

(Figure 1)**.** The peak at about 1740 cm^{-1} is due to the –NH–C=O carbonyl group, whereas the peak at 1462 cm^{-1} arises due to C=C bond. This bond was broken after sulfating process. The peak at 1377 cm^{-1} is due to S–O stretching absorption bands. FTIR spectrum showed that, the presence of –OH group after sulfating process. It indicates the almost complete removal of C=C bond by sulfating process and the process occur only on C=C.

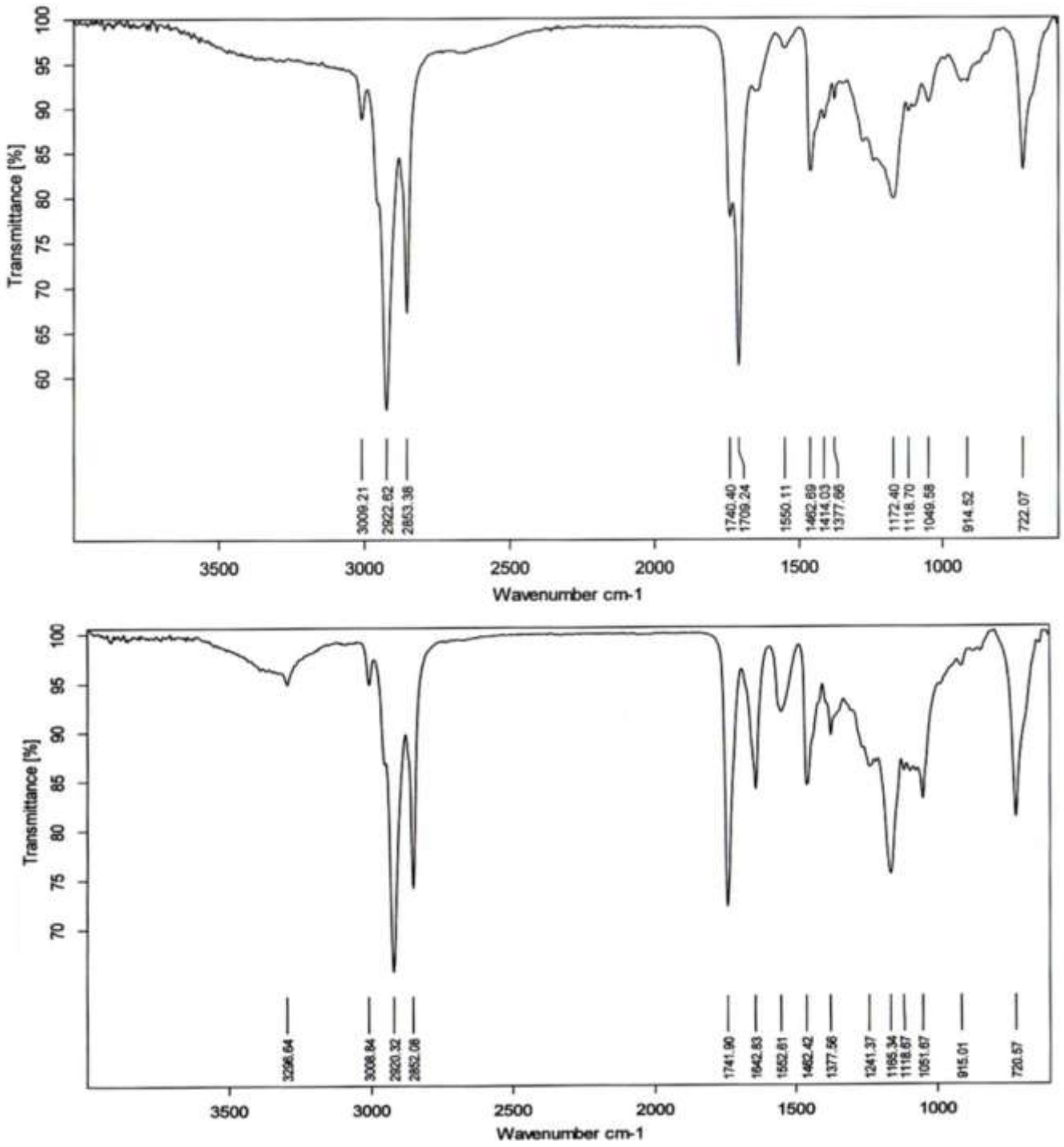

Figure 1. FTIR spectrum of (*a*) fatty acid monoethanolamine amide derived from cottonseed oil, (*b*) fatty acid diethanolamine amide after sulfating process.

The FT-IR for compound **V** showed an absorption band in the 2325 cm^{-1} region, indicating that formation ammonium ion ($-^{+}NH_2$) occurs. In addition, there was a strong band at 890 cm^{-1}, indicating the presence of multiple (CH_2) groups. The very strong band in the 2850 region was due mainly to the methyl asymmetric stretching vibration. The sharp band at 2925 cm^{-1} was observed for the investigated compounds due to the stretching vibration of the symmetric methylene group. The FT-IR absorption spectra confirmed the disappearance of −OH band of $-SO_2-OH$ (broad band), this confirmed the transfer of proton of acid to nitrogen atom of amine to form $-^{+}NH_2$ group. The results are generally in agreement with the expected correlations.

3.2. Potentiodynamic polarization measurements

Figure 2 shows the influence of inhibitors S_I and S_{II} concentrations on the Tafel cathodic and anodic polarization characteristics of mild steel in CO_2-saturted brine at a scan rate of 1 mV/s and at 50°C. Corrosion parameters were calculated on the basis of cathodic and anodic potential versus current density characteristics in the Tafel potential region [13, 14]. The values of the corrosion current density (I_{corr}) for the investigated metal without and with the inhibitor respectively were determined. It can be seen that the presence of surfactants molecule results a marked shift in both cathodic and anodic branches of the polarization curves towards lower current densities. This means that, the inhibitors affect both cathodic and anodic reactions. It was found that, both anodic and cathodic reactions of mild steel electrode corrosion were inhibited with increasing concentration of synthesized inhibitors. These results suggest that not only the addition of synthesized surfactants reduce anodic dissolution but also retard the hydrogen evolution reaction. The results showed that the inhibiting action of these inhibitors on the both cathodic and anodic processes seems to approximately be equal. The inhibitor may decrease the corrosion through the reduction of mild steel reactivity. Accordingly to this mechanism, a reduction of either the anodic or the cathodic reaction or both arises from the adsorption of the inhibitor on the corresponding active sites [15].

Steady state of open circuit corrosion potential (E_{corr}) for the investigated mild steel electrode in the presence and absence of the studied inhibitors was attained after 60–70 min from the moment of immersion. Corrosion current density (I_{corr}) of the investigated electrodes was determined, by extrapolation of cathodic and anodic Tafel lines to corrosion potential (E_{corr}). The inhibition efficiency expressed as percent inhibition (η%) is defined as:

$$\eta\% = \frac{I_{uninh} - I_{inh}}{I_{uninh}} \times 100 \quad (1)$$

where I_{uninh} and I_{inh} are the uninhibited and inhibited corrosion currents. The inhibited corrosion currents are those determined in the presence of the studied surfactants used in this investigation. The uninhibited corrosion currents were determined in pure (inhibitor free) CO_2-saturated 1% NaCl solution at the same temperature.

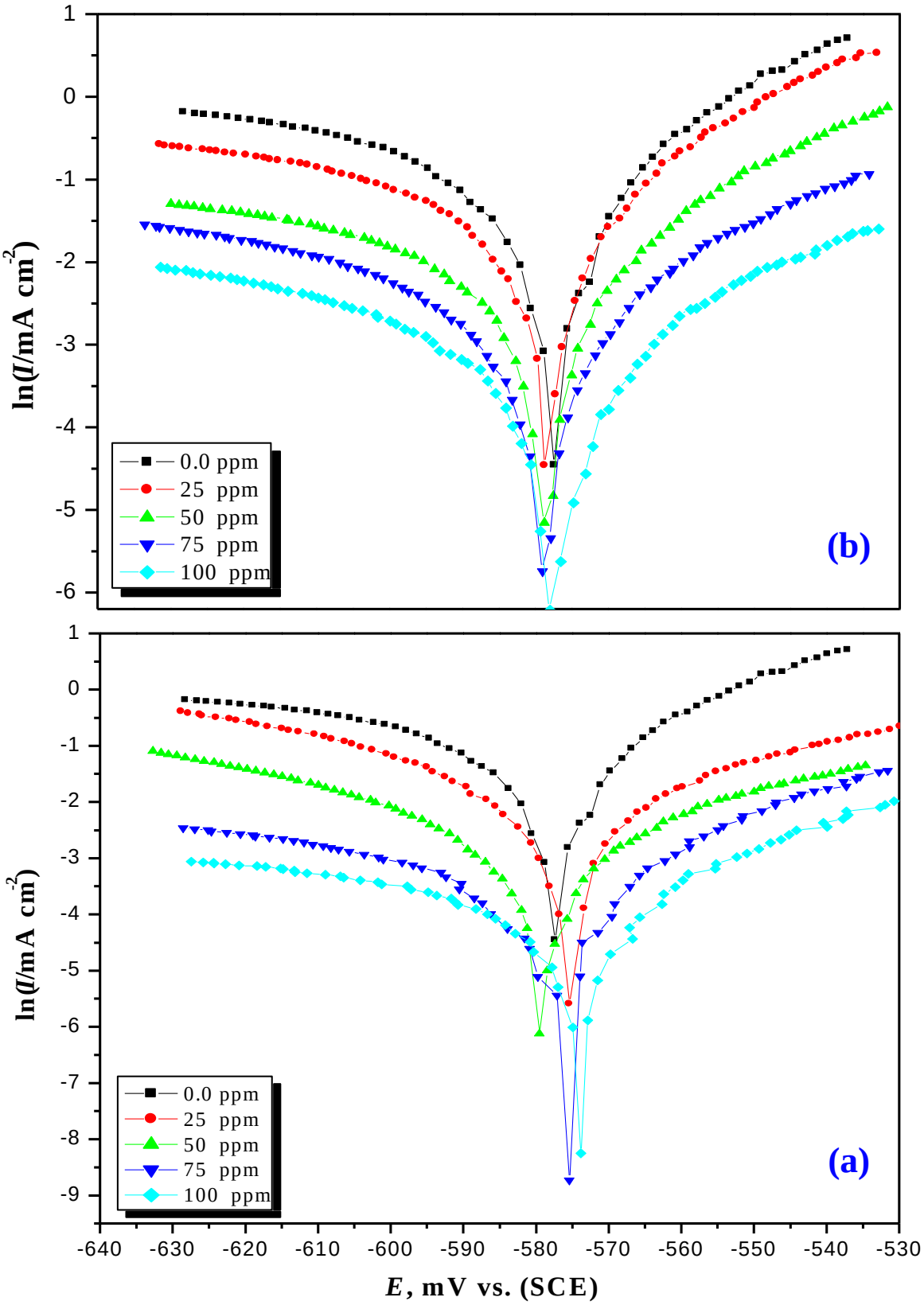

Figure 2. Polarization curves for the mild steel in CO_2-saturated 1% NaCl solution in absence and presence of different concentrations of surfactants S_I (*a*) and S_{II} (*b*) at 50 ºC.

The electrochemical parameters E_{corr}, I_{corr}, inhibition efficiency (η%), anodic and cathodic Tafel slopes (β_a, β_c) obtained from the polarization measurements were listed in Table 3. The data exhibited that, the corrosion current density (I_{corr}) decreases, and the inhibition efficiency (η%) increases as the inhibitor concentrations is increased. These results suggest that retardation of the electrodes processes occurs, at both cathodic and anodic sites, as a result of coverage of these sites by surfactants molecules. However, the maximum decrease in I_{corr} (0.013 mA cm^{-2}) was observed for (S_I). This could be attributed to the increase of the number of actives sites [16, 17]**.** The increase of inhibitor efficiency with increasing the concentration can be interpreted on the basis of the adsorption amount and the coverage of surfactants molecules, increases with increasing concentration [18]. The E_{corr} values of all synthesized inhibitors were shifted slightly toward both cathodic and anodic directions and did not show any definite trend in CO_2-saturated brine. This may be contributed to the mixed-type behavior of the studied inhibitors. It can be observed, the shift in E_{corr} that is characteristic of anodic and anodic/cathodic inhibitor [19]. It was explained that this shift in E_{corr} is due to active sites blocking effect that occurs when an inhibitor is added [20]. In the case of CO_2 corrosion the anodic and cathodic reactions are the oxidation of iron and the reduction of hydrogen, respectively [21]. If it is considered that the active sites on the metal surface are the same for both reactions before adding the inhibitor, it is logical the change in E_{corr} when the inhibitor is present because its adsorption change those active sites and therefore the anodic and cathodic reaction rates [22].

The fact that the slopes of the cathodic (β_c) and anodic (β_a) Tafel lines in Table 3 are approximately constant and independent of inhibitor concentration. These results indicate that this inhibitors act by simply blocking the available surface area. In other words, the inhibitor decreases the surface area for corrosion of the investigated metal, and only causes inactivation of a part of the surface with respect to corrosive medium [18]. On the other hand, the anodic Tafel slopes (β_a) are also found to be greater than the respective cathodic Tafel slopes (β_c). These observations are correlated with the fact that the anodic exchange-current density values are less than those of the cathodic counter parts. It can be concluded that the overall kinetics of corrosion of mild steel alloy in CO_2 saturated solution are under anodic control.

The high θ value (see Table 3) near unity indicates almost a full coverage of the metal surface with adsorbed surfactant molecules. Conclusively, the inhibitor having θ near unity is considered as a good physical barrier shielding the corroding surface from corrosive medium and dumping the corrosion rate of mild steel significantly. The high inhibition efficiencies are attributed to the high surface coverage of the inhibitor molecules. Data in Table 3 shows that the inhibition efficiency increased with increasing the inhibitor concentrations. The inhibition efficiency of the investigated inhibitors was increased in the following order: $S_I > S_{II} > S_V > S_{III} > S_{IV}$.

Table 3. Corrosion parameters obtained from potentiodynamic polarization for mild steel in CO_2 saturated 1% NaCl solution in the absence and presence of various concentrations of the surfactants at 50°C.

Inhibitor code	Conc. of inhibitor (ppm)	$-E_{corr}$ (mV *vs.* Ag/AgCl)	I_{corr} (mA cm^{-2})	β_a (mVdec^{-1})	$-\beta_c$ (mV dec^{-1})	θ	η,%
Absence	0.0	577	0.393	45	110	–	–
S_I	25	575	0.058	42	99	0.85	85.12
	50	579	0.037	35	100	0.90	90.52
	75	575	0.030	37	106	0.92	92.34
	100	573	0.013	39	104	0.96	96.44
S_{II}	25	577	0.049	38	103	0.87	87.43
	50	578	0.029	38	98	0.92	92.39
	75	578	0.018	41	101	0.95	95.21
	100	577	0.014	37	107	0.96	96.25
S_{III}	25	577	0.111	38	104	0.71	71.67
	50	575	0.079	43	101	0.79	79.89
	75	578	0.066	38	100	0.82	82.98
	100	575	0.057	36	98	0.85	85.28
S_{IV}	25	579	0.213	44	99	0.45	45.67
	50	580	0.180	41	106	0.54	54.05
	75	578	0.146	39	104	0.62	62.65
	100	574	0.116	36	103	0.70	70.34
S_V	25	579	0.115	35	99	0.70	70.57
	50	577	0.076	37	96	0.80	80.48
	75	576	0.059	39	99	0.84	84.78
	100	573	0.047	41	97	0.87	87.96

3.1. The linear polarization resistance (LPR) corrosion rate

Figures 3*a*, *b* and *c* show that the change in corrosion rate (CR) with time for mild steel in CO_2-saturated 1%NaCl solution containing different concentrations form inhibitors S_I, S_{II} and S_V at 50°C. The inhibitor was added after 1 hour of exposure because at this time the corrosion potential got stable, allowing the measurement of the CR prior the injection of the inhibitor. The initial corrosion rate, without inhibitor, was measured to be between 3.45 and 5.03 mm y^{-1}. It can be observed from Figure 3 that the CR, in the absence of inhibitor, tends to increase with time. The increase in CR has been attributed to the galvanic effect between the ferrite phase and cementite (Fe_3C) which is a part of the original steel in the non-oxidized state and accumulates on the surface after the preferential dissolution of

ferrite (α-Fe) into Fe^{2+} [23]. Fe_3C is known to be less active than the ferrite phase. Therefore, there is a preferential dissolution of ferrite over cementite, working the former as the anode and latter as the cathode, favoring the hydrogen evolved reaction (HER) during the corrosion process [24].

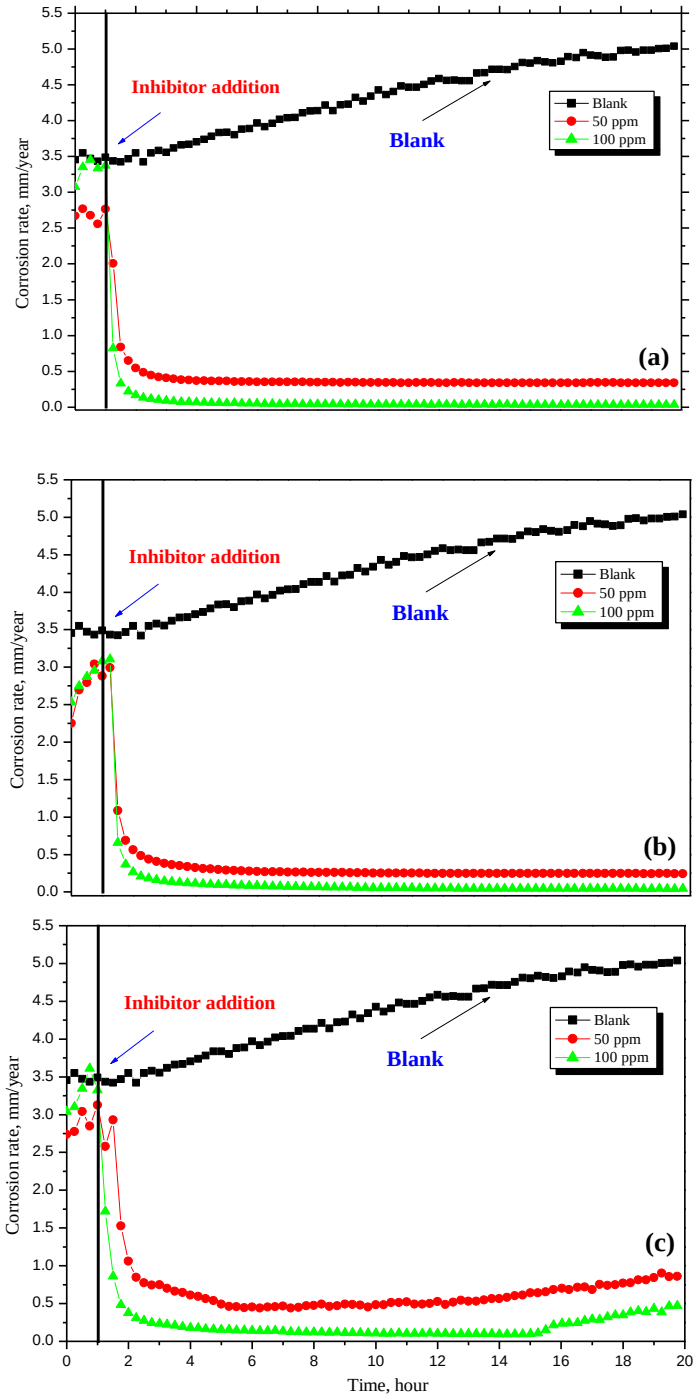

Figure 3. Variation of the corrosion rate with time for mild steel in CO_2-saturated brine containing different concentrations of inhibitors: $\mathbf{S_I}$ (*a*), $\mathbf{S_{II}}$ (*b*) and $\mathbf{S_V}$ (*c*) at 50°C.

Corrosion parameters were calculated on the basis of LPR corrosion rate test. The inhibition efficiency (η%) and surface coverage (θ) were calculated according to the following equations [9]:

$$\eta\% = \frac{CR_0 - CR_i}{CR_0} \times 100 \quad (2)$$

Surface coverage (θ):

$$\theta = 1 - \frac{CR_i}{CR_0} \quad (3)$$

where CR_0 is the corrosion rate without inhibitor and CR_i is the corrosion rate when inhibitor is present. It can be seen that the presence of inhibitors results in a high decrease in the rate of corrosion. In the case of these surfactants, the corrosion rate decreases as the inhibitor concentration increases, getting maximum inhibition efficiency ranged between 72.46 and 99.34% at 100 ppm after 20 hour of exposure. This trend may results from the fact that adsorption and surface coverage increase with the increase in concentration; thus the surface is effectively separated from the medium [25].

Table 4 shows the values of corrosion rates and the inhibition efficiencies in the presence of different concentrations of different inhibitors at 50°C. The data exhibited that, the corrosion rates and the inhibition are found to depend on the concentrations of the inhibitors. The corrosion rates (CR) are decreased, and the inhibition efficiencies (η%) and are increased with the increase of the surfactant concentrations. This indicates that the inhibitory action of the inhibitors against mild steel corrosion can be attributed to the adsorption of these molecules on the metal surface, limits the dissolution of mild steel, and the adsorption amounts of surfactants on mild steel increase with concentrations in the corrosive solutions.

Figure 4 shows the variation of the corrosion rate with time for mild steel in CO_2-saturated 1% NaCl solution containing 100 ppm from different investigated surfactants at 50 °C. This plot indicates that, the presence of all inhibitors decreases the rate of corrosion. However, the maximum decrease in the corrosion rate was observed for inhibitor (**S_I**) and the inhibition efficiency of the investigated surfactants was increased in the following order: $S_I > S_{II} > S_V > S_{III} > S_{IV}$. There was an increase in the efficiency of corrosion inhibition with increasing concentration, Due to their containment of C=O, oxygen, nitrogen and sulfur groups these molecules contribute towards inhibition, and effectively protect the surface. Adsorption of these surface active molecules forms thin inhibitor films on the metal surface which in order relatively isolate the metal surface from the corrosive environment causing much reduced corrosion rates. Inhibition efficiency of these films depends on various factors including but not limited to corrosivity of the environment, concentration of the active inhibitor molecules, any synergetic effects with other molecules present in the environment and/or flow/shear effects.

Table 4: The corrosion parameters obtained from LPR corrosion rate measurements for mild steel electrode in CO_2-saturated 1% solution of NaCl in the absence and presence of various concentrations of surfactants obtained based on cottonseed oil at 50°C.

Inhibitor code	Concentration, ppm	Corrosion rate, mm/year	Surface coverage, θ	The inhibition efficiency, η%
Blank	0.0	5.037	–	–
S_I	50	0.340	0.93	93.24
	100	0.033	0.99	99.34
S_{II}	50	0.243	0.95	95.17
	100	0.043	0.99	99.14
S_{III}	50	0.892	0.82	82.29
	100	0.612	0.87	87.84
S_{IV}	50	2.232	0.55	55.68
	100	1.387	0.72	72.46
S_V	50	0.861	0.82	82.90
	100	0.473	0.90	90.60

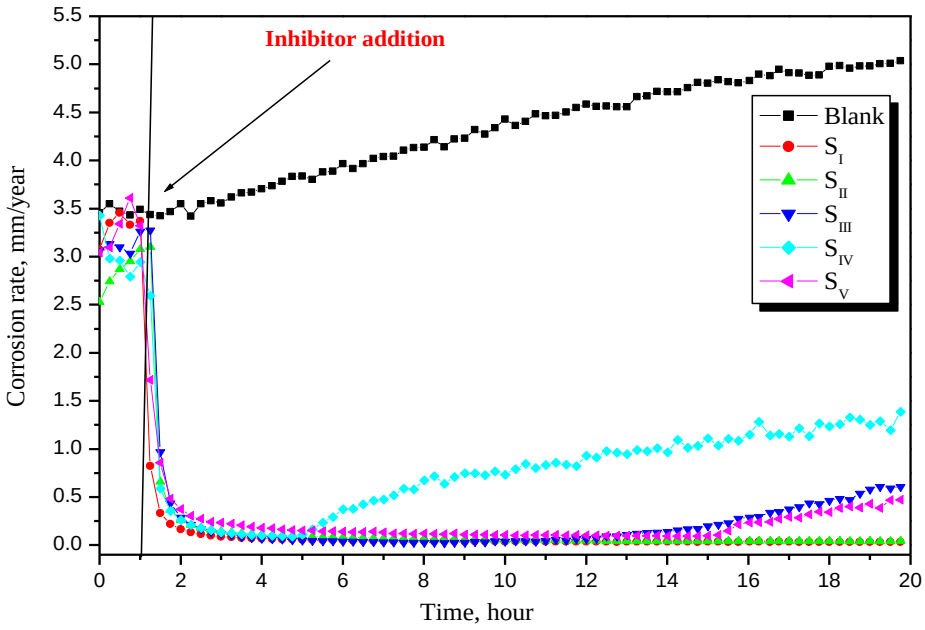

Figure 4. Variation of the corrosion rate with time for mild steel in CO_2-saturated brine containing 100 ppm from different surfactants at 50°C.

The high inhibition efficiency obtained in CO_2-saturated 1% NaCl solution in the presence of studied inhibitors can be attributed to the formation of a protective film of iron carbonate ($FeCO_3$) as follows [26]:

$$CO_{2(g)} \leftrightarrow CO_{2(aq)} \quad (4)$$

$$CO_{2(aq)} + H_2O \leftrightarrow H_2CO_{3(aq)} \quad (5)$$

$$H_2CO_{3(aq)} \leftrightarrow H^+ + HCO_3^- \quad (6)$$

$$HCO_3^- \leftrightarrow H^+ + CO_3^{2-} \quad (7)$$

The anodic dissolution for iron in carbonic acid solutions gives ferrous ions [26].

$$Fe \leftrightarrow Fe^{2+} + 2e^- \quad (8)$$

According to these processes, a corrosion layer was formed on the steel surface. The properties of the formed layers and its effect on the corrosion rate are important factors to take into account when studying the corrosion of steels in CO_2 environments. Ogundele and White suggested that iron carbonate, $FeCO_3$, may be important in the formation of protective layers on steel surface [27]. The formation of iron carbonate can be explained by using the following Eq. [28].

$$Fe^{2+} + CO_3^{2-} \rightarrow FeCO_3 \quad (9)$$

3.4. Adsorption isotherm and thermodynamic parameters for the corrosion process

Classical adsorption isotherms have been used extensively in the study of adsorption of organic surfactants onto mild steel electrode. It is widely acknowledged that they provide useful insights into the mechanism of corrosion inhibition [29]. Determination of the type of adsorption isotherm itself provides information on the adsorption process such as surface coverage, adsorption equilibrium constant and information on the interaction between the organic compound and electrode surface.

The interaction between the inhibitors and electrode surface can be described by the adsorption isotherm. During corrosion inhibition of metals and alloys, the nature of the inhibitor on the corroding surface has been deduced in terms of adsorption characteristics of the inhibitor. Furthermore, the solvent (H_2O) molecules could also be adsorbed at metal/solution interface. So the adsorption of surfactant molecules from aqueous solution can be regarded as a quasi-substitution process between the surfactant compounds in the aqueous phase [surfactant $_{(sol.)}$] and water molecules at the electrode surface [$H_2O_{(ads)}$] [30]:

$$\text{Surfactant}_{(sol.)} + nH_2O_{(ads.)} = \text{Surfactant}_{(ads.)} + nH_2O_{(sol.)} \quad (10)$$

where n is the size ratio, that is, the number of water molecules replaced by one organic inhibitor. Basic information on the interaction between the inhibitor and the electrode surface can be provided by the adsorption isotherm. In order to obtain the isotherm, the linear relation between the degree of surface coverage (θ) obtained from Tafel polarization

(θ = η%/100) and inhibitor concentration (C_i) must be found. Attempts were made to fit the θ values to various isotherms including Langmuir, Temkin, Frumkin and Flory–Huggins. By far the best fit was obtained with the Langmuir isotherm. The Langmuir isotherm is based on the assumption that all adsorption sites are equivalent and that particle binding occurs independently from nearby sites, whether occupied or not [31]. According to this isotherm, θ is related to C by:

$$\frac{C_{inh}}{\theta} = C_{inh} + \frac{1}{K_{ads}} \tag{11}$$

where K_{ads} is the equilibrium constant of the inhibitor adsorption process and C_{inh} is the inhibitor concentration.

Straight lines of C_i/θ versus C_i plots indicate that the adsorption of the inhibitor molecules on the electrode surface obeyed Langmuir adsorption model (Figure 5). The regression coefficients of the fitted curves are around unity ($R^2 > 0.9993$). The inhibition tendency of the tested inhibitors is due to the adsorption of this molecule on the electrode surface [32]. However, the slopes of the C_i/θ versus C_i plots are close to unity which indicates the ideal simulating for Langmuir adsorption isotherm (Table 5). K_{ads} values were calculated from the intercepts of the straight lines on the C_i/θ axis [33] and correlated to the standard free energy of adsorption (ΔG^o_{ads}) using the following equation [34]:

$$K_{ads} = \frac{1}{55.5}\exp\left(-\frac{\Delta G^0_{ads}}{RT}\right) \tag{12}$$

The value 55.5 in the above equation was the molar concentration of water in solution in mol/L [7]. The relatively high value of the adsorption equilibrium constant (K_{ads}; Table 5) reflects the high adsorption ability of these inhibitors on the electrode surface [35]. It is also noted that, the high value of K_{ads} for inhibitor S_I indicates stronger adsorption on the mild steel surface than the other inhibitors. Large values of K_{ads} imply more efficient adsorption hence better inhibition efficiency [36]. It is seen that the values of K_{ads} was increased in the following order: $S_I > S_{II} > S_V > S_{III} > S_{IV}$. These data are in a good agreement with that obtained from potentiodynamic polarization and LPR corrosion rate measurements.

Generally, values of ΔG^0_{ads} up to –20 kJ mol^{-1} are consistent with physisorption, while those around –40 kJ mol^{-1} or higher are associated with chemisorption as a result of the sharing or transfer of electrons from organic molecules to the metal surface to form a coordinate bond [37]. In the present study, The values of ΔG^0_{ads} obtained for studied surfactant inhibitors on mild steel in CO_2-saturated solution ranges between –36.31 and –41.91 kJ mol^{-1}, which are around –40 kJ mol^{-1} (Table 5). These results indicate that the adsorption mechanism of the investigated inhibitors on mild steel electrode is typical chemisorption at the studied temperature.

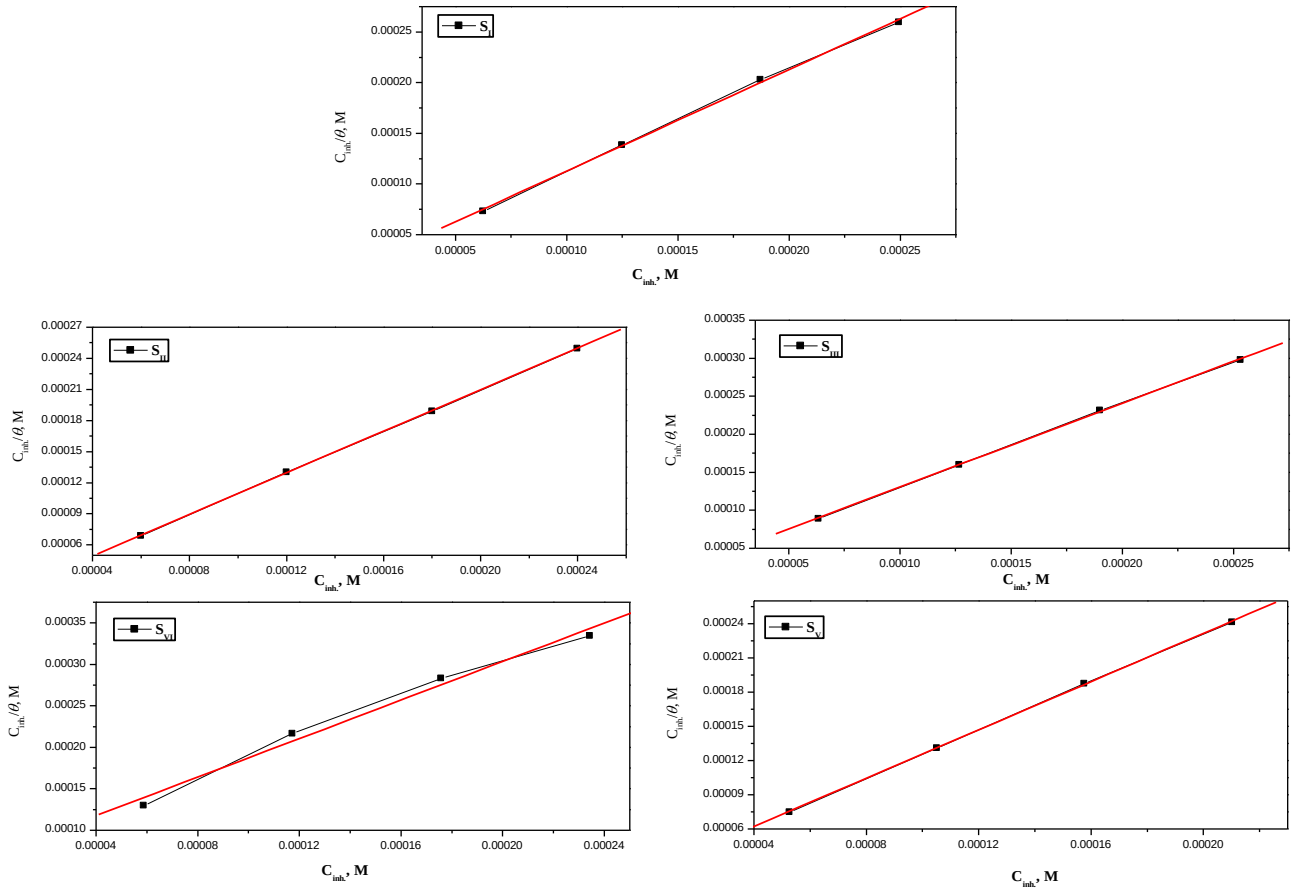

Figure 5. Langmuir adsorption isotherm (C_i/θ *vs.* C_i) fitting of the Tafel polarization data obtained for mild steel alloys in CO_2-saturated solution containing various concentrations of surfactants at 50°C.

Table 5. Thermodynamic parameters for the adsorption of the studied inhibitors on mild steel alloys in CO_2-saturated 1% NaCl solution at 50°C.

Inhibitor code	Slope	Regression coefficients, R^2	K_{ads}, $M^{-1} \times 10^4$	ΔG^0_{ads} (kJ mol^{-1})
S_I	1.0009	0.9994	10.90	–41.91
S_{II}	1.003	0.9999	7.87	–41.04
S_{III}	1.101	0.9998	4.91	–39.78
S_{IV}	1.160	0.9993	1.40	–36.31
S_V	1.050	0.9999	5.025	–39.83

3.5. Surface activity

It is well known that surfactants are characterized by critical micelle concentration (CMC). The CMC is the concentration where surfactants in solution change their initial molecular solvated state [6]. At this concentration, physical and chemical properties exhibit an abrupt variation. The surface tension *vs.* −log concentration profiles of the surfactant S_I (as example) showed two characteristic regions (Figure 6). The first at low concentrations and characterized by continuous decrease of the surface tension values due to the adsorption of surfactant molecules at the interface. The second region locates at higher surfactant concentrations where the surface tension values are almost stable. The intercept of these two regions gave the critical micelle concentration, CMC values [7]. It can be seen that the critical micelle concentration of S_I is 3.2×10^{-3} mol/l. It is known that highly dispersible, stable emulsion-like inhibitor solutions obtained at concentrations higher than CMC are more effective corrosion inhibitors than completely soluble inhibitor systems (below CMC).

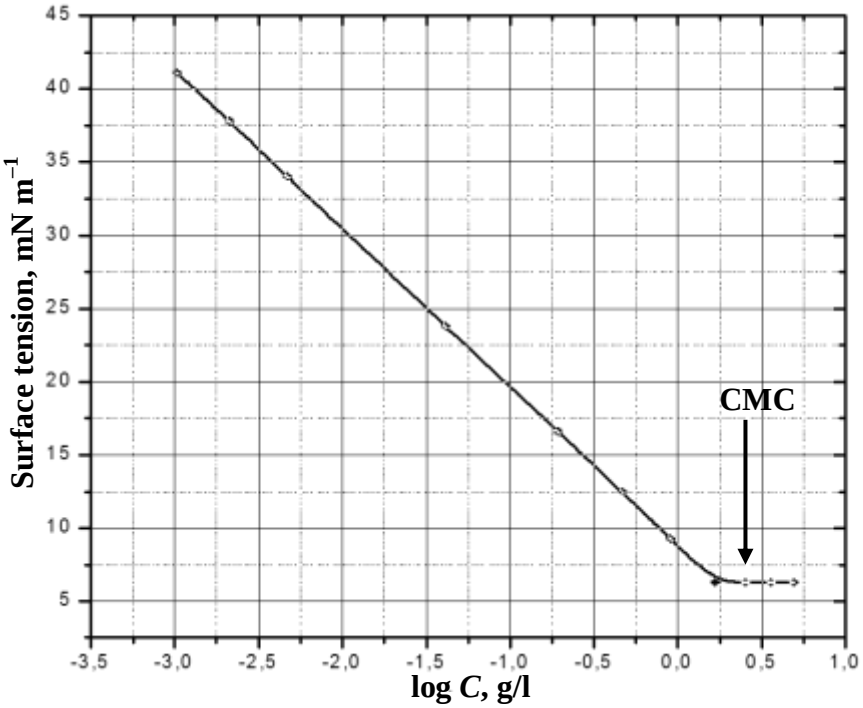

Figure 6. Surface tension versus concentration of inhibitor S_I in aqueous solution at 25°C.

4. Conclusion

In the above results and discussion, the following conclusions are drawn:

1. Green surfactants in the series of fatty acid amide were synthesized, and their surface activities were determined.
2. The corrosion inhibition efficiencies of the synthesized surfactants were studied by potentiodynamic polarization and linear polarization resistance corrosion rate measurements at 50°C, and they gave similar results.

3. Test results show that the surfactants studied are efficient inhibitors for mild steel corrosion in CO_2-saturated solution.
4. The inhibition efficiencies increase with the increase of inhibitor concentrations, which reveals the inhibitive actions of these inhibitors are mainly due to the adsorption on the electrode surface.
5. All surfactants showed predominantly mixed type behavior in CO_2-saturated brine.
6. The data obtained from the potentiodynamic polarization measurements for the studied inhibitors fit well into the Langmuir adsorption isotherm. The values of the free energy for the adsorption process indicate that chemisorption is involved in the adsorption of the studied fatty acid amide surfactants on the mild steel surface.

References

1. W. F. Rogers and J. A. Rowe, Jr., *Proc. Fourth World Petroleum Congress*, Rome, 1955, 479.
2. F. H. Meyer, O. L. Riggs, R. L. McGlasson and J. D. Sudbury, *Corrosion*, 1958, **14**, 109.
3. E. C. Greco and W. B. Wright, *Corrosion*, 1962, **18**, 119.
4. M. Bonis, M. Girgis, K. Goerz and R. MacDonald, *Corrosion/2006*, NACE International, Houston, Texas, 2006, paper no. 06122.
5. S. N. Smith and M. Joosten, Corrosion/2006, NACE International, Houston, Texas, 2006, paper no. 06115.
6. V. M. Abbasov, Hany M. Abd El-Lateef, L. I. Aliyeva, I. T. Ismayilov and E. E. Qasimov, *J. Korean Chem. Soc.*, 2013, **57**, no. 1, 25.
7. I. T. Ismayilov, Hany M. Abd El-Lateef, V. M. Abbasov, L. I. Aliyeva, E. N. Efremenko, S. A. Mamedxanova, *Int. Res. J. of Pure & Appl. Chem.*, 2014, **4**, no. 3, 299.
8. Hany M. Abd El-Lateef, V. M. Abbasov, L. I. Aliyeva, E. E. Qasimov and I. T. Ismayilov, *Mater. Chem. Phys*., 2013, **142**, 502.
9. I. T. Ismayilov, Hany M. Abd El-Lateef, V. M. Abbasov, S. A. Mamedxanova, U. C. Yolchuyeva and Ch. K. Salmanova, *Am. J. Appl. Chem*., 2013, **1**, no. 5, 79.
10. Hany M. Abd El-Lateef, I. T. Ismayilov, V. M. Abbasov, E. N. Efremenko, L. I. Aliyeva and E. E. Qasimov, *Am. J. Phys. Chem*., 2013, **2**, no. 1, 16.
11. R. Fuchs-Godec, *Acta Chim. Slov*., 2007, **54**, 492.
12. M. El Azhar, B. Mernari, M. Traisnel, F. Bentiss and M. Lag-renée, *Corros. Sci*., 2001, **43**, 2229.
13. R. Tremont, H. De Jesus-Cardona, J. Garcia-Orozco, R. J. Castro and C. R. Cabrera, *J. Appl. Electrochem*., 2000, **30**, 737.
14. J. W. Schultze and K. Wippermann, *Electrochim. Acta*, 1987, **32**, 823.
15. M. S. Abdel Aal, A. A. Abdel Wahab and A. El-Sayed, *Corrosion*, 1981, **37**, 557.
16. A. A. El-Shafei, S. A. And El-Maksoud and A. S. Fouda, *Corros. Sci*., 2004, **46**, 579.

17. E. Akbarzadeh, M. N. M. Ibrahim and A. A. Rahim, *Int. J. Electrochem. Sci*., 2011, **6**, 5396.
18. A. El-Sayed, Hossnia S. Mohran and H. M. Abd El-Lateef, *Corros. Sci*., 2010, **52**, 1976.
19. D. A. López, S. N. Simison and S. R. de Sánchez, *Corros. Sci*., 2005, **47**, 735.
20. C. Cao, *Corros. Sci*., 1996, **38**, 2073.
21. M. Nordsveen, S. Nesic, R. Nyborg and A. Stangelend, *Corrosion*, 2003, **59**, 443.
22. F. Farelas and A. Ramirez, *Int. J. Electrochem. Sci*., 2010, **5**, 797.
23. J. Crolet, N. Thevenot and S. Nesic, *Corrosion*, 1998, **54**, 194.
24. K. Videm, J. Kvarekvaal, T. Perez and G. Fitzsimons, *Corrosion/96*, NACE International, Houston, Texas, 1996, paper No. 1.
25. A. El-Sayed, A. M. Shaker and H. M. Abd El-Lateef, *Corros. Sci*., 2010, **52**, 72.
26. D. A. Lo´pez, S.N. Simison and S.R. de Sa´nchez, *Electrochim. Acta*, 2003, **48**, 845.
27. G. I. Ogundele and W. E. White, *Corrosion*, 1986, **42**, 71.
28. M. A. Migahed, M. Abd-El-Raouf, A. M. Al-Sabagh and H. M. Abd-El-Bary, *J. Appl. Electrochem*., 2006, **36**, 395.
29. W. Durnie, R. De Marco, A. Jefferson and B. Kinsella, *J. Electrochem. Soc*., 1999, **146**, 1751.
30. M. Sahin, S. Bilgic and H. Yilmaz, *Appl. Surf. Sci*., 2002, **195**, 1.
31. R. Solmaz, G. Kardas, M. Culha, B. Yazici and M. Erbil, *Electrochim. Acta*, 2008, **53**, 5941.
32. I. B. Obot and N. O. Egbedi, *Port. Electrochim. Acta*, 2009, **27**, 517.
33. F. Tang, X. Wang, X. Xu and L. Li, *Colloids Surf. A*, 2010, **369**, 101.
34. J. Flis and T. Zakroczymski, *J. Electrochem. Soc*., 1996, **143**, 2458.
35. S. A. Refay, F. Taha and A. M. Abd El-Malak, *Appl. Surf. Sci*., 2004, **236**, 175.
36. V. Branzoi, F. Branzoi and M. Baibarac, *Mater. Chem. Phys*., 2000, **65**, 288.
37. S. Bilgic and M. Sahin, *Chem. Phys*., 2001, **70**, 290.

♦ ♦ ♦